Published for SISSA by Springer

Received: *September 12, 2024*
Revised: *November 20, 2024*
Accepted: *November 26, 2024*
Published: *December 11, 2024*

Modular flavored dark matter

Alexander Baur[a,b] **Mu-Chun Chen**[c] **V. Knapp-Pérez**[c] **and Saúl Ramos-Sánchez**[a]

[a] *Instituto de Física, Universidad Nacional Autónoma de México, Cd. de México C.P. 04510, Mexico*
[b] *Physik Department, Technische Universität München, James-Franck-Straße 1, 85748 Garching, Germany*
[c] *Department of Physics and Astronomy, University of California, Irvine, CA 92697-4575, U.S.A.*

E-mail: alexander.baur@tum.de, muchunc@uci.edu, vknapppe@uci.edu, ramos@fisica.unam.mx

Abstract: Discrete flavor symmetries have been an appealing approach for explaining the observed flavor structure, which is not justified in the Standard Model (SM). Typically, these models require a so-called flavon field in order to give rise to the flavor structure upon the breaking of the flavor symmetry by the vacuum expectation value (VEV) of the flavon. Generally, in order to obtain the desired vacuum alignment, a flavon potential that includes additional so-called driving fields is required. On the other hand, allowing the flavor symmetry to be modular leads to a structure where the couplings are all holomorphic functions that depend only on a complex modulus, thus greatly reducing the number of parameters in the model. We show that these elements can be combined to simultaneously explain the flavor structure and dark matter (DM) relic abundance. We present a modular model with flavon vacuum alignment that allows for realistic flavor predictions while providing a successful fermionic DM candidate.

Keywords: Discrete Symmetries, Flavour Symmetries, Models for Dark Matter

ArXiv ePrint: 2409.02178

https://doi.org/10.1007/JHEP12(2024)091

JHEP12(2024)091

Contents

1 Introduction

The origin of the mass hierarchies and mixings among the three generations of fermions is unexplained in the Standard Model (SM). One possible solution to address this so-called flavor puzzle is the introduction of *traditional flavor symmetries* that allow for transformations among fermions of different flavors. These symmetries are independent of moduli and are known to provide explanations for the flavor structure of both the lepton and quark sectors [1–7]. To achieve these results, models endowed with traditional flavor symmetries require the introduction of two kinds of extra SM singlet scalars: i) flavons, whose vacuum expectation value (VEV)s are responsible for the non-trivial flavor structure of fermions, and ii) driving fields [8–15] that help to shape a suitable potential for obtaining the desired VEV pattern. The traditional flavor symmetry framework based on non-Abelian discrete symmetries has also proven helpful for dark matter (DM), where the flavor symmetry plays the role of a stabilizer symmetry [16]. Furthermore, (not necessarily discrete) flavor symmetries can be successfully combined to explain both DM and flavor anomalies from SM decays [17–19].

Another promising approach to explain the flavor parameters without introducing many scalars is provided by so-called modular flavor symmetries [20–29]. This approach has produced good fits for leptons [22, 25, 28, 30–41] and quarks [24, 42–53]. In this scenario, instead of depending on flavon VEVs, Yukawa couplings are replaced by multiplets of modular forms depending on the half-period ratio τ, which can be considered a complex modulus. The basic problem then reduces to explaining why τ stabilizes at its best-fit value $\langle\tau\rangle$, for which being close to the symmetry-enhanced points $\tau = \mathrm{i}$, $\mathrm{e}^{2\pi\mathrm{i}/3}$, $\mathrm{i}\infty$ can be advantageous [54–58]. Although this scheme has the potential to avoid the need for any additional scalar field, the presence of flavons in addition to the modulus can be useful too (see, e.g., Model 1 of [20] and [21]). Similarly to the traditional flavor case, modular flavor symmetries can also serve as stabilizer symmetries for DM candidates [59–63]

JHEP12(2024)091

Modular flavor symmetries arise naturally in top-down constructions, such as magnetized extra dimensions [64–77] or heterotic string orbifolds [78–89], where they combine with traditional flavor symmetries, building an eclectic flavor group [90]. Remarkably, these top-down approaches provide a natural scheme where not only realistic predictions arise [88], but also the modulus τ can be stabilized close to symmetry-enhanced points [91–97].

Motivated by these observations, we propose a new supersymmetric model combined with modular flavor symmetries, which simultaneously accomplishes the following:

1. Addressing the flavor puzzle, specifically the origin of the lepton masses and mixing parameters;

2. Achieving the vacuum alignment for the flavons;

3. Providing a suitable DM candidate with the correct observed DM abundance, $\Omega_{\rm DM} = 0.265(7)$ [98].

In order to tackle these issues, we propose a simple supersymmetric model based on a $\Gamma_3 \cong A_4$ modular flavor symmetry. The model resembles Model 1 of [20], where the neutrino masses arise from a Weinberg operator and the charged-lepton Yukawa couplings are given by the VEV of a flavon. It also resembles the proposal of [99], which studies a DM candidate in a non-modular A_4 model without fitting flavor parameters. In our model, the flavon potential is fixed by the flavor symmetry together with a $\mathrm{U}(1)_{\rm R} \times \mathbb{Z}_2$ symmetry, which determines the couplings between the driving field and flavon superfields. The model gives a very good fit to the leptonic flavor parameters, with a low value of χ^2. Finally, we identify a Dirac fermion composed by the Weyl fermionic parts of both the driving field and flavon superfields; we perform a parameter scan for a correct DM abundance. The goal of this model is to present a "proof of principle" that driving fields in modular supersymmetric flavor models can account for both the flavon VEV $\langle\phi\rangle$ and DM.

Our paper is organized as follows. In section 2, we review the basics of modular symmetries and its application to solving the flavor puzzle. In section 3, we define our model. In section 4, we present the numerical fit for the lepton flavor parameters. In section 5, we analyze the relevant terms for DM production. We also argue why we need freeze-in (as opposed to the more traditional freeze-out) mechanism for our model to work. We then present a parameter scan for the available parameter space for our DM candidate. Finally, in section 6 we summarize our results and future directions for further constraints.

2 Modular symmetry

2.1 Modular groups and modular forms

The modular group $\Gamma := \mathrm{SL}(2,\mathbb{Z})$ is given by

$$\Gamma \;=\; \left\{ \begin{pmatrix} a & b \\ c & d \end{pmatrix} \;\middle|\; a,b,c,d \in \mathbb{Z} \;\&\; ad-bc=1 \right\} , \tag{2.1}$$

JHEP12(2024)091

and can be generated by

$$S \;=\; \begin{pmatrix} 0 & 1 \\ -1 & 0 \end{pmatrix} \qquad \text{and} \qquad T \;=\; \begin{pmatrix} 1 & 1 \\ 0 & 1 \end{pmatrix} , \tag{2.2}$$

which satisfy the general presentation of Γ, $\langle S, T \mid S^4 = (ST)^3 = \mathbb{1}, S^2T = TS^2 \rangle$. The principle congruence subgroups of level N of Γ are defined as

$$\Gamma(N) \;:=\; \{\gamma \in \Gamma \mid \gamma = \mathbb{1} \mod N\} , \tag{2.3}$$

which are infinite normal subgroups of Γ with finite index. We can also define the inhomogeneous modular group $\overline{\Gamma} := \Gamma/\{\pm\mathbb{1}\} \cong \mathrm{PSL}(2,\mathbb{Z})$ and its subgroups $\overline{\Gamma}(N)$ with $\overline{\Gamma}(2) := \Gamma(2)/\{\pm\mathbb{1}\}$ and $\overline{\Gamma}(N) := \Gamma(N)$ for $N > 2$ (as $-\mathbb{1}$ does not belong to $\Gamma(N)$). An element γ of a modular group acts on the half-period ratio, modulus τ, as

$$\gamma\,\tau \;=\; \frac{a\tau + b}{c\tau + d} , \qquad \text{where} \quad \tau \in \mathcal{H} \tag{2.4}$$

and $\mathcal{H}$ is the upper complex half-plane,

$$\mathcal{H} \;:=\; \{\tau \in \mathbb{C} \mid \mathrm{Im}\,\tau > 0\} . \tag{2.5}$$

Modular forms $f(\tau)$ of positive modular weight k and level N are complex functions of τ, holomorphic in $\mathcal{H}$, and transform as

$$f(\tau) \;\xrightarrow{\gamma}\; f(\gamma\,\tau) \;=\; (c\tau + d)^k\, f(\tau) , \qquad \gamma \in \Gamma(N) . \tag{2.6}$$

In this work, we restrict ourselves to even modular weights, $k \in 2\mathbb{N}$, although it is known that modular weights can be odd [28] or fractional [72, 100] in certain scenarios. Interestingly, modular forms with fixed weight k and level N build finite-dimensional vector spaces, which close under the action of Γ. It follows then that they must build representations of a finite modular group that, for even modular weights, result from the quotient

$$\Gamma_N \;:=\; \overline{\Gamma}/\overline{\Gamma}(N) . \tag{2.7}$$

Then, under a finite modular transformation $\gamma \in \Gamma$, modular forms of weight k are n-plets (which are called vector-valued modular forms [101]) $Y(\tau) := (f_1(\tau), f_2(\tau), \ldots, f_n(\tau))^{\mathrm{T}}$ of Γ_N, transforming as

$$Y(\tau) \;\xrightarrow{\gamma}\; Y(\gamma\,\tau) \;=\; (c\tau + d)^k\, \rho(\gamma)\, Y(\tau) , \tag{2.8}$$

where $\rho(\gamma) \in \Gamma_N$ is a representation of γ.

2.1.1 Finite modular group $\Gamma_3 \cong A_4$

As our model is based on $\Gamma_3 \cong A_4$, let us discuss some general features of this group and its modular forms. Γ_3 is defined by the presentation

$$\Gamma_3 \;=\; \Big\langle S, T \mid S^2 \;=\; (ST)^3 \;=\; T^3 \;=\; \mathbb{1} \Big\rangle . \tag{2.9}$$

JHEP12(2024)091

	$\mathbf{1}$	$\mathbf{1'}$	$\mathbf{1''}$	$\mathbf{3}$		$\mathbf{1}$	$\mathbf{1'}$	$\mathbf{1''}$	$\mathbf{3}$
$\rho(S)$	1	1	1	$\frac{1}{3}\begin{pmatrix}-1 & 2 & 2\\ 2 & -1 & 2\\ 2 & 2 & -1\end{pmatrix}$	$\rho(T)$	1	ω	ω^2	$\begin{pmatrix}1 & 0 & 0\\ 0 & \omega & 0\\ 0 & 0 & \omega^2\end{pmatrix}$

Table 1. Irreducible representations of $\Gamma_3 \cong A_4$. Here, $\omega := \mathrm{e}^{2\pi\mathrm{i}/3}$.

It has order 12 and the irreducible representations (in the complex basis) are given in table 1. Besides $\mathbf{1}^a \otimes \mathbf{1}^b = \mathbf{1}^c$ with $c = a + b \mod 3$ and $\mathbf{1}^a \otimes \mathbf{3} = \mathbf{3}$, where $a, b, c = 0, 1, 2$ count the number of primes, we have the nontrivial product rule $\mathbf{3} \otimes \mathbf{3} = \mathbf{1} \oplus \mathbf{1'} \oplus \mathbf{1''} \oplus \mathbf{3}_S \oplus \mathbf{3}_A$, where S and A stand respectively for symmetric and antisymmetric. Considering two triplets $\rho = (\rho_1, \rho_2, \rho_3)^{\mathrm{T}}$ and $\psi = (\psi_1, \psi_2, \psi_3)^{\mathrm{T}}$, in our conventions the Clebsch-Gordan coefficients of $\rho \otimes \psi$ are

$$
\begin{aligned}
&(\rho\otimes\psi)_{\mathbf{1}} = \rho_1\psi_1 + \rho_2\psi_3 + \rho_3\psi_2\,, \qquad (\rho\otimes\psi)_{\mathbf{1'}} = \rho_1\psi_2 + \rho_2\psi_1 + \rho_3\psi_3\,,\\
&(\rho\otimes\psi)_{\mathbf{1''}} = \rho_1\psi_3 + \rho_2\psi_2 + \rho_3\psi_1\,,\\
&(\rho\otimes\psi)_{\mathbf{3}_S} = \frac{1}{\sqrt{3}}\begin{pmatrix}2\rho_1\psi_1 - \rho_2\psi_3 - \rho_3\psi_2\\ 2\rho_3\psi_3 - \rho_1\psi_2 - \rho_2\psi_1\\ 2\rho_2\psi_2 - \rho_3\psi_1 - \rho_1\psi_3\end{pmatrix}, \quad (\rho\otimes\psi)_{\mathbf{3}_A} = \begin{pmatrix}\rho_2\psi_3 - \rho_3\psi_2\\ \rho_1\psi_2 - \rho_2\psi_1\\ \rho_3\psi_1 - \rho_1\psi_3\end{pmatrix}.
\end{aligned}
\tag{2.10}
$$

The lowest-weight modular forms of Γ_3 furnish a triplet $Y = (Y_1, Y_2, Y_3)^{\mathrm{T}}$ of weight $k_Y = 2$, whose components are given by [20]

$$
\begin{aligned}
Y_1(\tau) &= \frac{\mathrm{i}}{2\pi}\left[\frac{\eta'\left(\frac{\tau}{3}\right)}{\eta\left(\frac{\tau}{3}\right)} + \frac{\eta'\left(\frac{\tau+1}{3}\right)}{\eta\left(\frac{\tau+1}{3}\right)} + \frac{\eta'\left(\frac{\tau+2}{3}\right)}{\eta\left(\frac{\tau+2}{3}\right)} - \frac{27\eta'(3\tau)}{\eta(3\tau)}\right],\\
Y_2(\tau) &= -\frac{\mathrm{i}}{\pi}\left[\frac{\eta'\left(\frac{\tau}{3}\right)}{\eta\left(\frac{\tau}{3}\right)} + \omega^2\frac{\eta'\left(\frac{\tau+1}{3}\right)}{\eta\left(\frac{\tau+1}{3}\right)} + \omega\frac{\eta'\left(\frac{\tau+2}{3}\right)}{\eta\left(\frac{\tau+2}{3}\right)}\right],\\
Y_3(\tau) &= -\frac{\mathrm{i}}{\pi}\left[\frac{\eta'\left(\frac{\tau}{3}\right)}{\eta\left(\frac{\tau}{3}\right)} + \omega\frac{\eta'\left(\frac{\tau+1}{3}\right)}{\eta\left(\frac{\tau+1}{3}\right)} + \omega^2\frac{\eta'\left(\frac{\tau+2}{3}\right)}{\eta\left(\frac{\tau+2}{3}\right)}\right],
\end{aligned}
\tag{2.11}
$$

where $\eta(\tau)$ is the so-called Dedekind η function

$$
\eta(\tau) \;=\; q^{1/24}\prod_{n=1}^{\infty}(1-q^n) \qquad \text{with} \qquad q := \mathrm{e}^{2\pi\mathrm{i}\tau}\,. \tag{2.12}
$$

Higher-weight modular forms can be constructed from the tensor products of the weight 2 modular forms given in eq. (2.11).

2.2 Modular supersymmetric theories

We consider models with $\mathcal{N} = 1$ *global* supersymmetry (SUSY), defined by the Lagrange density

$$
\mathcal{L} \;=\; \int \mathrm{d}^2\theta\,\mathrm{d}^2\bar{\theta}\,K(\Phi,\overline{\Phi}) + \left(\int \mathrm{d}^2\,\theta\,W(\Phi) + \mathrm{h.c.}\right), \tag{2.13}
$$

JHEP12(2024)091

where $K(\Phi,\overline{\Phi})$ is the Kähler potential, $W(\Phi)$ is the superpotential, and Φ denotes collectively all matter superfields φ^i of the theory and the modulus τ.

Under an element of the modular symmetry $\gamma \in \Gamma$, τ transforms according to eq. (2.4), and matter superfields are assumed to transform as

$$\varphi^i \quad \xrightarrow{\gamma} \quad (c\tau+d)^{-k_i}\rho_i(\gamma)\,\varphi^i\,, \tag{2.14}$$

where k_i are also called modular weights of the field φ^i, which transform as Γ_N multiplets. Modular weights k_i are not restricted to be positive integers because φ^i are not modular forms. Analogous to eq. (2.8), the matrix $\rho_i(\gamma)$ is a representation of the finite modular flavor group Γ_N.

For simplicity, we assume a minimal Kähler potential[1] of the form

$$K(\Phi,\overline{\Phi}) \;=\; -\log(-\mathrm{i}\tau+\mathrm{i}\bar{\tau})+\sum_i(-\mathrm{i}\tau+\mathrm{i}\bar{\tau})^{-k_i}|\varphi^i|^2\,. \tag{2.15}$$

Making use of eq. (2.14), we see that $K(\Phi,\overline{\Phi})$ transforms under a modular transformation $\gamma \in \Gamma$ as

$$K(\Phi,\overline{\Phi}) \quad \xrightarrow{\gamma} \quad K(\Phi,\overline{\Phi})+\log(c\tau+d)+\log(c\bar{\tau}+d)\,. \tag{2.16}$$

Thus, realizing that the Kähler potential is left invariant up to a *global* supersymmetric Kähler transformation, in order for the Lagrange density of eq. (2.13) to be modular invariant, we need the superpotential to be invariant under modular transformations, i.e.

$$W(\Phi) \quad \xrightarrow{\gamma} \quad W(\Phi)\,. \tag{2.17}$$

The superpotential $W(\Phi)$ has the general form

$$W(\Phi) \;=\; \mu_{ij}(\tau)\varphi^i\varphi^j+Y_{ijk}(\tau)\varphi^i\varphi^j\varphi^k+G_{ijk\ell}(\tau)\varphi^i\varphi^j\varphi^k\varphi^\ell\,, \tag{2.18}$$

where $\mu_{ij}(\tau)$, $Y_{ijk}(\tau)$ and $G_{ijk}(\tau)$ are modular forms of level N. Because of eq. (2.17), each term of eq. (2.18) must be modular invariant. Let us illustrate how we can achieve this by taking the trilinear coupling $Y_{ijk}(\tau)\varphi^i\varphi^j\varphi^k$. The Yukawa coupling Y_{ijk} transforms under a modular transformation $\gamma \in \Gamma$ as

$$Y_{ijk}(\tau) \quad \xrightarrow{\gamma} \quad (c\tau+d)^{k_Y}\rho_Y(\gamma)\,Y_{ijk}(\tau)\,, \tag{2.19}$$

where k_Y is the even integer modular weight of the modular form $Y_{ijk}(\tau)$. Then, for $Y_{ijk}(\tau)\varphi^i\varphi^j\varphi^k$ to be invariant and using the superfield transformations of eq. (2.14), we must demand that $k_Y = k_i+k_j+k_k$ and that the product $\rho_Y\otimes\rho_i\otimes\rho_j\otimes\rho_k$ contains an invariant singlet.

Since we shall be concerned with SUSY breaking, let us briefly discuss the soft-SUSY breaking terms in the Lagrange density. They are given by

$$\mathcal{L}_{\text{soft}} \;=\; -\frac{1}{2}\left(M_a\hat{\lambda}^a\hat{\lambda}^a+\text{h.c}\right)-\tilde{m}_i^2\bar{\hat{\varphi}}^i\hat{\varphi}^i-\left(A_{ijk}\hat{\varphi}^i\hat{\varphi}^j\hat{\varphi}^k+B_{ij}\hat{\varphi}^i\hat{\varphi}^j+\text{h.c.}\right)\,, \tag{2.20}$$

[1] In principle, there could be further terms in the Kähler potential with an impact on the flavor predictions [102], which are ignored here.

JHEP12(2024)091

	L	(E_1^c, E_2^c, E_3^c)	H_d	H_u	ϕ_3	$\phi_{1'}$	ζ_3	$\zeta_{1''}$	$Y(\tau)$
$\mathrm{SU}(2)_L$	**2**	**1**	**2**	**2**	**1**	**1**	**1**	**1**	**1**
$\mathrm{U}(1)_Y$	$-\frac{1}{2}$	1	$-\frac{1}{2}$	$\frac{1}{2}$	0	0	0	0	0
$\Gamma_3 \cong A_4$	**3**	$(\mathbf{1}, \mathbf{1''}, \mathbf{1'})$	**1**	**1**	**3**	**1′**	**3**	**1″**	**3**
k_i	1	0	-1	0	0	0	0	0	2
$\mathrm{U}(1)_R$	1	1	0	0	0	0	2	2	0
$\mathbb{Z}_2$	0	0	0	0	0	-1	0	-1	0

Table 2. Quantum numbers under the SM gauge groups, $\mathrm{U}(1)_R$, $\mathbb{Z}_2$ and Γ_3, as well as modular weights k_i of the matter fields in our model. All fields are neutral under $\mathrm{SU}(3)_{\mathrm{color}}$.

where M_a are the gaugino masses, $\hat{\lambda}^a$ are the canonically normalized gaugino fields, and $\tilde{m}_i$ are the soft-masses. We use a notation, where $\hat{\varphi}^i$ stands for both the canonically normalized chiral superfield and its scalar component [103]. We do not assume any specific source of SUSY breaking, and thus the parameters in eq. (2.20) are free, in principle. However, in our model $B-$terms are forbidden at tree level and the A-terms do not play a role in DM production at tree-level, see section 5.

3 Dark modular flavon model

We propose a model of leptons, governed by the modular flavor group $\Gamma_3 \cong A_4$. In our model, the lepton doublets L transform as a flavor triplet and charged-lepton singlets E_i^c transform as three distinct singlets under Γ_3. The particle content of our model is summarized in table 2.

In our model, neutrino masses arise from the Weinberg operator

$$W_\nu \;=\; \frac{1}{\Lambda}\left(H_u L H_u L Y(\tau)\right)_{\mathbf{1}} \;, \tag{3.1}$$

where Λ is the neutrino-mass scale and $Y(\tau)$ is the modular-form triplet $Y = (Y_1, Y_2, Y_3)^{\mathrm{T}}$ of weight 2 given by eq. (2.11). Note that there exists no other modular multiplet of weight 2 in $\Gamma_3 \cong A_4$. Hence, under our assumptions, the neutrino sector obtained from eq. (3.1) is highly predictive as it only depends on the parameter τ, the VEV v_u of H_u, and Λ.

The charged-lepton superpotential at leading order is

$$W_{\mathrm{CL}} \;=\; \frac{\alpha_1}{\Lambda_\phi} E_1^c H_d (L\phi_3)_{\mathbf{1}} + \frac{\alpha_2}{\Lambda_\phi} E_2^c H_d (L\phi_3)_{\mathbf{1'}} + \frac{\alpha_3}{\Lambda_\phi} E_3^c H_d (L\phi_3)_{\mathbf{1''}} \;, \tag{3.2}$$

where α_i, $i = 1, 2, 3$, are dimensionless parameters, Λ_ϕ denotes the flavor breaking scale, and the subindices refer to the respective Γ_3 singlet components of tensored matter states in the parentheses. The charged-lepton mass matrix can be determined by the Γ_3 triplet flavon VEV $\langle\phi_3\rangle$ as in Model 1 of [20]. However, we have taken a different value of $\langle\phi_3\rangle$, which eventually leads to a better fit.

JHEP12(2024)091

The flavon superpotential is given by

$$W_\phi = \Lambda_\phi \beta_1 \zeta_3 \phi_3 + \beta_2 \zeta_3 \phi_3 \phi_3 + \frac{\beta_3}{\Lambda_\phi} \zeta_3 \phi_3 \phi_3 \phi_3 + \Lambda_\phi \beta_4 \zeta_{1''} \phi_{1'} + \frac{\beta_5}{\Lambda_\phi} \zeta_{1''} \phi_{1'} \phi_3 \phi_3 + \frac{\beta_6}{\Lambda_\phi} \zeta_3 \phi_3 \phi_{1'} \phi_{1'} \,, \tag{3.3}$$

where β_i, $i = 1, \ldots, 6$, are dimensionless couplings. This superpotential gives rise to the desired VEV pattern with driving superfields ζ_r, $r = 1'', 3$, and an extra flavon $\phi_{1'}$, where the subindices label the respective A_4 representations. To fix the flavon superpotential, we impose a symmetry $\mathrm{U}(1)_\mathrm{R} \times \mathbb{Z}_2$, similarly to [8, 99]. As usual, the $\mathrm{U}(1)_\mathrm{R}$ R-symmetry forbids the renormalizable terms in the superpotential that violate lepton and/or baryon numbers. We remark that the flavon superpotential eq. (3.3) is important for both finding the correct vacuum alignment for the flavons, as discussed below, and for identifying a viable DM candidate as described in section 5.

The flavon VEV is then attained by demanding that SUSY remains unbroken at a first stage, i.e. we require vanishing F-terms. Recall that the F-term scalar potential in a global supersymmetric theory is given schematically by

$$V \;=\; F^i K_{i\bar{j}} \bar{F}^{\bar{j}} \,, \tag{3.4}$$

where

$$F^i = -\frac{\partial W}{\partial \Phi^i} \,, \qquad \bar{F}^{\bar{j}} = F^{j*} \qquad \text{and} \qquad K^{i\bar{j}} = (K_{i\bar{j}})^{-1} = (-\mathrm{i}\tau + \mathrm{i}\tau)^{k_i} \delta_{i\bar{j}} \,. \tag{3.5}$$

Recall that a superfield Φ can be expanded in its components as [104, Equation 2.117]

$$\Phi = \Phi(x) - \mathrm{i}\theta\sigma^\mu\bar{\theta}\partial_\mu\Phi(x) - \frac{1}{4}\theta^2\bar{\theta}^2\partial^2\Phi(x) + \sqrt{2}\theta\psi_\Phi(x) + \frac{\mathrm{i}}{\sqrt{2}}\theta^2\partial_\mu\psi_\Phi(x)\sigma^\mu\bar{\theta} + \theta^2 F_\Phi(x) \,, \tag{3.6}$$

where we have used the notation that Φ represents both the superfield and its scalar component, ψ_Φ is the fermionic component and F_Φ is the F-term. For SUSY to be preserved, we must have $\langle F_\Phi \rangle = 0$. We assume that the only possible sources of SUSY breaking are given either by τ or a hidden sector. Thus, we demand $\left\langle F_{\varphi^i} \right\rangle = 0$, for all i, where φ^i represents the matter fields in our model (cf. eq. (2.13)). We solve these F-term equations at the VEV's of the flavons ϕ_3 and $\phi_{1'}$ and Higgs fields,

$$\langle \phi_3 \rangle =: v_3 \, (1, a, b)^T \,, \qquad \langle \phi_{1'} \rangle =: v_{1'} \,, \qquad \langle H_u \rangle =: v_u \qquad \text{and} \qquad \langle H_d \rangle =: v_d \,. \tag{3.7}$$

where we assume $a, b, v_3, v_{1'} \in \mathbb{R}$. All F-term equations are trivially satisfied except the ones corresponding to the driving fields given by

$$\langle F_{\zeta_{3i}} \rangle \;=\; 0 \qquad \text{and} \qquad \langle F_{\zeta_{1''}} \rangle \;=\; 0 \,, \tag{3.8}$$

where ζ_{3i}, $i = 1, 2, 3$, are the three components of the triplet. Thus, we obtain the following relations

$$\begin{aligned} \beta_2 &= c_2(a,b)\beta_1 \frac{\Lambda_\phi}{v_3} \,, & \beta_3 &= c_3(a,b)\beta_1 \frac{\Lambda_\phi^2}{v_3^2} \,, \\ \beta_5 &= c_5(a,b)\beta_4 \frac{\Lambda_\phi^2}{v_3^2} \,, & \beta_6 &= c_6(a,b)\beta_1 \frac{\Lambda_\phi^2}{v_{1'}^2} \,, \end{aligned} \tag{3.9}$$

where $c_i(a,b)$, for $i = 2,3,5,6$, are coefficients that depend only on the values of a, b. The numerical values of a, b dictate the charged lepton mass matrix. Hence, they are determined by the fit to the flavor parameters that we do in section 4. Through the flavor parameter fit, we have found values of $\langle\phi_3\rangle, \langle\phi_{1'}\rangle$ that satisfy simultaneously eq. (3.9), thus yielding vacuum alignment.

Finally, we assume that the flavon VEV scale from eq. (3.7) is below Λ_ϕ, such that

$$v_3 \;=\; v_{1'} \;=\; 0.1\Lambda_\phi \,. \tag{3.10}$$

Furthermore, we identify the DM candidate as a Dirac fermion built as a combination of the Weyl components of ζ_i and ϕ_i with the scalar component of the flavon ϕ_i serving as a mediator. The parameters in eq. (3.10) shall play an important role in finding the current DM abundance since they set the couplings in eq. (3.3).

4 Flavor fit

Having defined our model of modular flavored dark matter, we next assess its capability to reproduce the experimentally observed charged-lepton masses, neutrino squared mass differences, and the mixing parameters of the PMNS matrix while providing predictions for yet undetermined observables, such as the three absolute neutrino masses, the Dirac $\mathcal{CP}$ phase, and the two Majorana phases.

The explicit neutrino mass matrix can be determined from eq. (3.1). By calculating the tensor products to obtain the symmetry invariant part, we find that the neutrino mass matrix is predicted to be

$$M_\nu \;=\; \frac{v_u^2}{\Lambda}\begin{pmatrix} 2Y_1 & -Y_3 & -Y_2 \\ -Y_3 & 2Y_2 & -Y_1 \\ -Y_2 & -Y_1 & 2Y_3 \end{pmatrix}. \tag{4.1}$$

The charged-lepton mass matrix M_{CL} arises from eq. (3.2). Substituting the flavon VEVs as defined in eq. (3.7) and calculating the tensor products, we arrive at

$$M_{\mathrm{CL}} \;=\; \frac{v_d v_3}{\Lambda_\phi}\begin{pmatrix} \alpha_1 & \alpha_1 b & \alpha_1 a \\ \alpha_2 a & \alpha_2 & \alpha_2 b \\ \alpha_3 b & \alpha_3 a & \alpha_3 \end{pmatrix} \;=\; 0.1 v_d \begin{pmatrix} \alpha_1 & \alpha_1 b & \alpha_1 a \\ \alpha_2 a & \alpha_2 & \alpha_2 b \\ \alpha_3 b & \alpha_3 a & \alpha_3 \end{pmatrix}, \tag{4.2}$$

where we have used eq. (3.10). The values of v_u and v_d are determined by the Higgs VEV, $v = \sqrt{v_u^2 + v_d^2} = 246\,\mathrm{GeV}$, and $\tan\beta = \frac{v_u}{v_d}$, which we assume to be $\tan\beta = 60$. The neutrino mass scale is determined by Λ, while we choose α_3 to set the mass scale of charged leptons. By using the standard procedure (see e.g. ref. [98]), one arrives at the lepton masses and the PMNS mixing matrix. For our model, the resulting 12 flavor observables depend on 6 real dimensionless parameters $\mathrm{Re}\,\tau$, $\mathrm{Im}\,\tau$, a, b, α_1/α_3, and α_2/α_3, as well as two dimensionful overall mass scales v_u^2/Λ and $0.1 v_d \alpha_3$.

To show that the model can accommodate the observed flavor structure of the SM lepton sector, we scan its parameter space and compare the resulting flavor observables to

JHEP12(2024)091

observables	best-fit values
m_e/m_μ	0.00473 ± 0.00004
m_μ/m_τ	0.0450 ± 0.0007
y_τ	0.795 ± 0.012
$\Delta m^2_{21}/10^{-5}$ [eV^2]	$7.41^{+0.21}_{-0.20}$
$\Delta m^2_{32}/10^{-3}$ [eV^2]	$-2.487^{+0.027}_{-0.024}$
$\sin^2\theta_{12}$	$0.307^{+0.012}_{-0.011}$
$\sin^2\theta_{13}$	$0.02222^{+0.00069}_{-0.00057}$
$\sin^2\theta_{23}$	$0.568^{+0.016}_{-0.021}$
$\delta^\ell_{\mathcal{CP}}/\pi$	$1.52^{+0.13}_{-0.15}$

Table 3. Experimental central values and 1σ uncertainties for the masses and mixing parameters of the lepton sector. The data for the neutrino oscillation parameters is taken from the global analysis NuFIT v5.3 [105] for inverted ordering taking the Super-Kamiokande data into account. The charged-lepton mass ratios and the tau Yukawa coupling y_τ are taken from ref. [106] with $M_{\rm SUSY} = 10\,\text{TeV}$, $\tan\beta = 60$, and $\bar{\eta}_b = 0$.

experimental data, with the best-fit values shown in table 3. As an approximate measurement of the goodness of our fit, we introduce a χ^2 function

$$\chi^2 \;=\; \sum_i \chi_i^2\,, \tag{4.3}$$

consisting of a quadratic sum of one-dimensional chi-square projections for each observable. Here, we assume that the uncertainties of the fitted observables are independent of each other and do not account for the small correlations among experimental errors of $\sin^2\theta_{23}$ and other quantities. For the mixing angles and the neutrino squared mass differences, we determine the value of χ_i^2 directly from the one-dimensional projections determined by the global analysis NuFIT v5.3 [105], which are available on their website. This is necessary to account for the strong non-Gaussianities in the uncertainties of the mixing parameters in the PMNS matrix. For these observables, we refrain from considering corrections from renormalization group running, given that their contribution is expected to be small compared to the size of the experimental errors. For the charged-lepton masses, we determine the value of χ_i^2 by

$$\chi_i \;=\; \frac{\mu_{i,\text{exp.}} - \mu_{i,\text{model}}}{\sigma_i}\,, \tag{4.4}$$

where $\mu_{i,\text{model}}$ denotes the resulting value for the ith observable of the model, while $\mu_{i,\text{exp.}}$ and σ_i refer to its experimentally observed central value and the size of the 1σ uncertainty interval given in table 3, respectively. The total value of χ^2 for all considered observables may then be interpreted to indicate an agreement with the experimental data at a $\sqrt{\chi^2}\,\sigma$ confidence level (C.L.).

To scan the parameter space of the model and minimize the χ^2 function, we use the dedicated code `FlavorPy` [107]. We find that the model is in agreement with current

JHEP12(2024)091

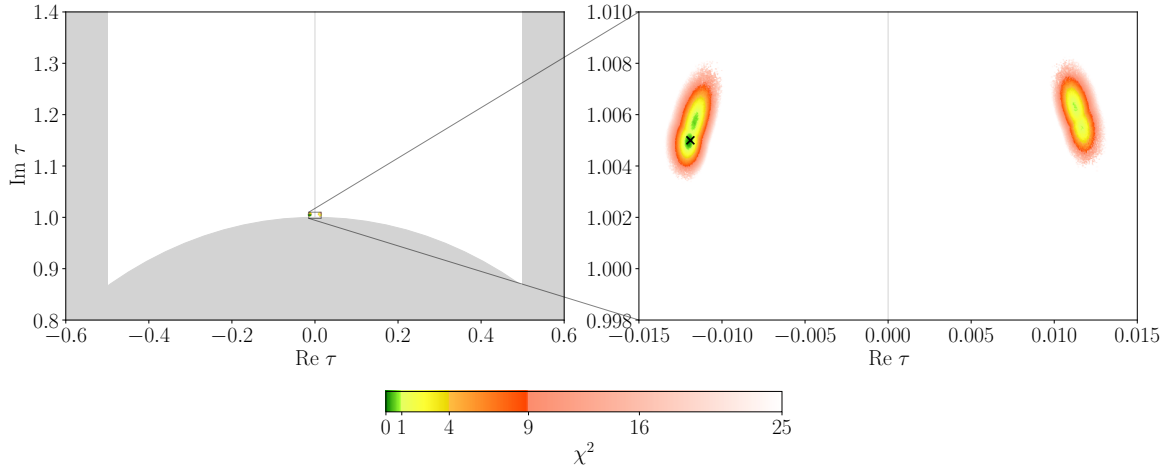

Figure 1. Regions in moduli space that yield fits with $\chi^2 \leq 25$. The green, yellow, and orange colored regions may be interpreted as the 1σ, 2σ, and 3σ confidence intervals, respectively, while the opaque red fades out until the 5σ barrier is reached. The best-fit point of eq. (4.5) is marked by ×. The unshaded area corresponds to the fundamental domain of $\mathrm{SL}(2,\mathbb{Z})$.

experimental observations. The best-fit point in the parameter space of our model is at

$$\begin{aligned} &\tau = -0.0119 + 1.005\mathrm{i}\,, \qquad a = -0.392\,, \qquad b = 0.380\,, \qquad 0.1\alpha_3 v_d = 0.130\,\mathrm{GeV} \\ &\frac{\alpha_1}{\alpha_3} = -22.0\,, \qquad \frac{\alpha_2}{\alpha_3} = 4.78\times 10^{-3}\,, \qquad \frac{v_u^2}{\Lambda} = 0.0221\,\mathrm{eV}\,, \end{aligned} \tag{4.5}$$

where we obtain $\chi^2 = 0.08$, meaning that all resulting observables are within their experimental 1σ interval, cf. also eq. (4.7). In figure 1, we present the regions in moduli space that yield results with $\chi^2 \leq 25$.

For the specific values given in eq. (4.5), the relations among the couplings of the flavon superpotential of eq. (3.9) read

$$\beta_2 = 4.27\beta_1\,, \qquad \beta_3 = 83.5\beta_1\,, \qquad \beta_5 = 142\beta_4\,, \qquad \beta_6 = 121\beta_1\,. \tag{4.6}$$

Any values of β_1 and β_4 then solve the F-term equations of the driving fields, cf. eq. (3.8), and ensure the specific vacuum alignment of eq. (4.5). The resulting observables at the best-fit point given in eq. (4.5) lie well within the 1σ intervals of the experimental data shown in table 3, and read

$$\begin{aligned} m_\mathrm{e}/m_\mu &= 0.00473\,, & m_\mu/m_\tau &= 0.0451\,, & y_\tau &= 0.795\,, \\ \sin^2\theta_{12} &= 0.306\,, & \sin^2\theta_{13} &= 0.02231\,, & \sin^2\theta_{23} &= 0.568\,, \\ \delta^\ell_{\mathcal{CP}}/\pi &= 1.52\ \mathrm{rad}\,, & \eta_1/\pi &= 1.41\ \mathrm{rad}, & \eta_2/\pi &= 0.351\ \mathrm{rad}\,, \\ m_1 &= 49\,\mathrm{meV}\,, & m_2 &= 50\,\mathrm{meV}\,, & m_3 &= 0.75\,\mathrm{meV}\,. \end{aligned} \tag{4.7}$$

Moreover, the resulting sum of neutrino masses, the neutrino mass observable in ^{3}H beta decay, and the effective neutrino mass for neutrinoless double beta decay, are

$$\sum m_i = 100\,\mathrm{meV}\,, \qquad m_\beta = 50\,\mathrm{meV}\,, \qquad \text{and} \qquad m_{\beta\beta} = 48\,\mathrm{meV}\,, \tag{4.8}$$

JHEP12(2024)091

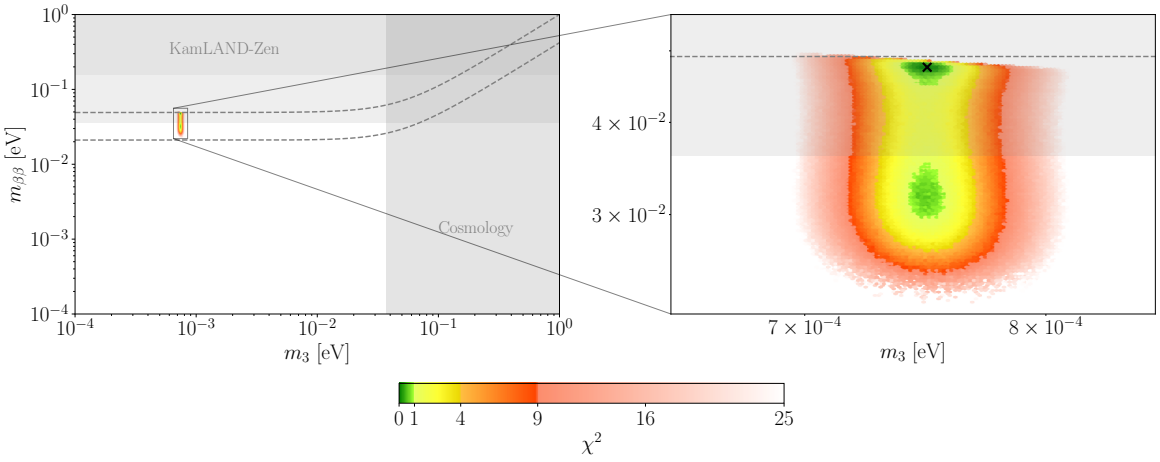

Figure 2. The effective neutrino mass for neutrinoless double beta decay as a function of the lightest neutrino mass. The experimentally allowed region within 3σ for inverted ordering is the region between the two dashed lines, while the region allowed in our model is represented by the colored area. The gray-shaded areas are excluded by KamLAND-Zen [110] or cosmological bounds [108, 111]. We remark that the KamLAND-Zen upper limit for the effective neutrino mass $m_{\beta\beta}$ depends on the used nuclear matrix element estimate. While all estimates applied by the KamLAND-Zen collaboration give rise to an upper bound of the effective mass to be below 156 meV (dark gray area), only some estimates yield limits that are smaller than 36 meV (light gray area) [110]. Hence, we find that the sample point marked by × is only challenged by some nuclear matrix element estimates while still being allowed according to the majority of estimates.

which are consistent with their latest experimental bounds $\sum m_i < 120\,\text{meV}$ [108], $m_\beta < 800\,\text{meV}$ [109], and $m_{\beta\beta} < 156\,\text{meV}$ [110]. It is to be noted that our predicted value of the effective neutrino mass $m_{\beta\beta}$ is challenged by experimental bounds determined with certain nuclear matrix element estimates [110], as illustrated in figure 2.

We remark that the model can be consistent with both octants of θ_{23}, while only being compatible with Dirac $\mathcal{CP}$-violating phases in the range of $1.36 < \delta^\ell_{\mathcal{CP}} < 1.55$ at a 3σ C.L., as shown in figure 3. Moreover, the inverted-ordering neutrino masses are predicted to lie within the narrow ranges

$$48\,\text{meV} < m_1 < 50\,\text{meV}\,, \quad 49\,\text{meV} < m_2 < 51\,\text{meV}\,, \quad 0.72\,\text{meV} < m_3 < 0.78\,\text{meV}\,, \quad (4.9)$$

at a 3σ C.L. The numerical analysis suggests that the model prefers a neutrino spectrum with inverted ordering. For a normal-ordering spectrum we only obtain a match with experimental data just barely in the 3σ interval with $\chi^2 \approx 7$.

5 DM abundance

Let us start by identifying the DM candidate. Since the flavon field only couples to charged leptons, the phenomenological implications for DM in our model are determined by the charged-lepton Yukawa interactions and the flavon potential. The interactions between the

JHEP12(2024)091

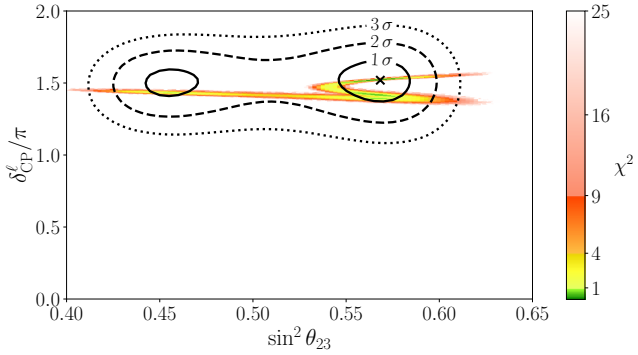

Figure 3. Predicted regions in the space of $\sin^2\theta_{23}$ and $\delta^\ell_{\mathcal{CP}}$ with $\chi^2 \leq 25$ in our model. The black lines indicate the regions that are experimentally admissible at a 1, 2, and 3σ C.L. as obtained by the global analysis NuFIT v5.3 [105].

SM charged leptons and the flavon scalar ϕ_3 are given by

$$\begin{aligned}\mathcal{L}_{\rm CL} &= -\sum_{i=1}^{3}\frac{v_d}{2}\alpha_i\,\psi_{E_i^C}\,(\psi_E\phi_3)_{\mathbf{1}} + \text{h.c} \\ &\longrightarrow -\sum_{i=1}^{3}\frac{v_d}{2}\alpha_i\,\psi_{E_i^C}\left(\psi_E\left(\phi_3 + v_3(1,a,b)^T\right)\right)_{\mathbf{1}} + \text{h.c.}\,,\end{aligned} \tag{5.1}$$

where ψ_E denotes the fermionic part of the charged-lepton component of L. In the last line, we develop the flavon ϕ_3 in the vacuum with its VEV given by $v_3(1,a,b)^T$, see eq. (3.7). From the leading flavon superpotential terms in eq. (3.3),[2] we obtain

$$\begin{aligned}\mathcal{L}_\phi &= -\frac{1}{2}\Lambda_\phi\beta_1\,(\psi_{\zeta_3}\psi_{\phi_3})_{\mathbf{1}} - \frac{1}{2}\beta_2\,(\psi_{\zeta_3}\psi_{\phi_3}\phi_3)_{\mathbf{1}} - \frac{1}{2}\Lambda_\phi\beta_4\left(\psi_{\zeta_{1''}}\psi_{\phi_{1'}}\right)_{\mathbf{1}} + \text{h.c.} \\ &\to -\frac{1}{2}\Lambda_\phi\beta_1\,(\psi_{\zeta_3}\psi_{\phi_3})_{\mathbf{1}} - \frac{1}{2}\beta_2\left(\psi_{\zeta_3}\psi_{\phi_3}\left(\phi_3 + v_3(1,a,b)^T\right)\right)_{\mathbf{1}} \\ &\quad -\frac{1}{2}\Lambda_\phi\beta_4\left(\psi_{\zeta_{1''}}\psi_{\phi_{1'}}\right)_{\mathbf{1}} + \text{h.c.} \\ &= -\frac{1}{2}\Lambda_\phi\beta_1\,(\psi_{\zeta_3}\psi_{\phi_3})_{\mathbf{1}} - \frac{4.27}{2}\beta_1\left(\psi_{\zeta_3}\psi_{\phi_3}\left(\phi_3 + v_3(1,a,b)^T\right)\right)_{\mathbf{1}} \\ &\quad -\frac{1}{2}\Lambda_\phi\beta_4\left(\psi_{\zeta_{1''}}\psi_{\phi_{1'}}\right)_{\mathbf{1}} + \text{h.c.}\,,\end{aligned} \tag{5.2}$$

where ϕ_3 is again expanded around its VEV in the second line and we use the relations of eq. (4.6) in the last line.

The DM candidate is the lowest mass-state Dirac fermion built as a linear combination of the Weyl components of the driving fields and flavon fields, $\psi_{\zeta_i}, \psi_{\phi_i}$, whereas the mediator is a linear combination of the flavon scalars. The particle content relevant for DM production is outlined in table 4. After the Higgs and the flavons acquire VEVs as given in eq. (3.7),[3] the symmetry group of table 2 gets broken down to $\mathrm{U}(1)_{\rm EM} \times \mathrm{U}(1)_R$.

[2] We ignore the terms suppressed by Λ_ϕ.

[3] The reheating temperature is chosen to be $T_{\rm R} = 150\,\text{GeV}$ such that DM production begins after Electroweak (EW) symmetry breaking. Recall that the EW symmetry breaking temperature of crossover is around 160 GeV with a width of 5 GeV [112]. We acknowledge that higher reheating temperatures are also possible, in which case, the production of DM happens before EW symmetry breaking. We leave this possibility for future work.

JHEP12(2024)091

	ψ_{E_i}	$\psi_{E_i^C}$	$\phi_{3,i}$	$\phi_{1'}$	$\psi_{\phi_{3,i}}$	$\psi_{\zeta_{3,i}}$	$\psi_{\phi_{1'}}$	$\psi_{\zeta_{1''}}$
$\mathrm{U}(1)_{\mathrm{EM}}$	-1	$+1$	0	0	0	0	0	0
$\mathrm{U}(1)_R$	0	0	0	0	-1	$+1$	-1	$+1$

Table 4. Particle content for DM production.

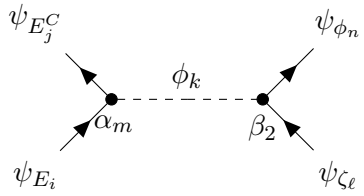

(a) DM production diagram.

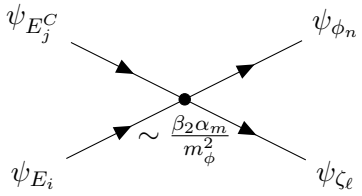

(b) Effective DM production diagram.

Figure 4. (a). The indices i, j, m indicate the three possible charged-lepton flavor states, while the indices n, k, ℓ indicate the three possible components of the triplet plus the non-trivial singlet of flavons and driving fields. DM is identified as the lowest mass-state of $\psi_{\zeta_\ell}, \psi_{\phi_n}$. The mediator is the scalar flavon ϕ_k. (b) Since the effective mass of the flavon scalar is expected to be very big, $m_\phi \gg m_{E_i}, m_{\psi_{\phi\zeta}}$, then the diagram shrinks to an effective 4−fermion interaction. This leads to a preferred freeze-in scenario.

Interactions in eqs. (5.1) and (5.2) allow for processes as shown in the diagrams in figure 4(a). Furthermore, we also consider the scalar potential

$$V = \frac{\partial W}{\partial \varphi_i} K^{i\bar{j}} \frac{\partial W^*}{\partial \varphi_{\bar{j}}^*} + \sum_{i=1,2,3} |\widetilde{m}_\phi \phi_{3,i}|^2 + |\widetilde{m}_\phi \phi_{1'}|^2 \,, \tag{5.3}$$

where we have added the soft-masses $\widetilde{m}_\phi$ for the flavon scalars. We assume that $\widetilde{m}_\phi$ is the same for the four scalars and should be of order of the SUSY breaking scale. It has been shown in [113] that for modular A_4 supersymmetric models, the SUSY breaking scale is constrained to be above 6 TeV. Therefore, we choose values of order $\widetilde{m}_\phi = 20 - 1000$ TeV. Furthermore, the A-term in eq. (2.20) does not play a significant role in DM production at tree-level since the production of DM through flavon scalar annihilations are suppressed due to the low reheating temperature we consider; therefore, we also ignore the A-term in our analysis.

It turns out that the correct DM relic abundance can be obtained with a freeze-in scenario [114] in this model (cf. [99] where a freeze-out production mechanism is utilized). This can be seen as follows. First, note that the effective scalar flavon mass m_ϕ is obtained by diagonalizing the mass matrix obtained from eq. (5.3). If we assume that $\widetilde{m}_\phi \gg m_{E_i}, m_{\psi_{\phi\zeta}}$, where $m_{E_i}, m_{\psi_{\phi\zeta}} = m_{\mathrm{DM}} \sim \Lambda_\phi \beta_1$ represent the mass of the charged leptons and the DM respectively, then the mediator mass ($m_\phi \sim \widetilde{m}_\phi + m_{\psi_{\phi\zeta}}$) is much larger than the DM and the charged-lepton masses. Therefore, the diagram figure 4(a) reduces to the effective 4−fermion operator as indicated in figure 4(b) with a coupling of $\sim \frac{\beta_2 \alpha_m}{m_\phi^2}$. In a freeze-out mechanism, if the rate $\langle \sigma v \rangle$ at which DM is annihilated decreases, then the amount of DM relic abundance increases. Since we must require $\beta_2 \ll 4\pi$ to retain perturbativity, and we expect $\alpha_1 = -6.97$,

JHEP12(2024)091

as explained at the end section 4, then

$$\langle \sigma v \rangle \sim \left| \frac{\beta_2 \alpha_m}{m_\phi^2} \right|^2 \ll \left| \frac{88}{m_\phi^2} \right|^2 . \tag{5.4}$$

Using `micrOMEGAs` 5.3.41 [115–117], we find that for the chosen values of Λ_ϕ and $\widetilde{m}_\phi$, too much DM is produced. Since increasing m_ϕ or lowering β_2 would only decrease $\langle \sigma v \rangle$, the DM abundance can not be decreased to the observed DM abundance in a freeze-out scenario.[4] On the other hand, for a freeze-in scenario, we have the opposite behavior. Specifically, if $\langle \sigma v \rangle$ decreases, the amount of produced DM also decreases. So, we can choose smaller β_2 or larger m_ϕ values to obtain the observed relic abundance of DM in the Universe.

We now proceed to present the predictions of our model for the DM abundance after performing a parameter scan. We use `micrOMEGAs` 5.3.41 [115–117] for the DM abundance computation and FeynRules 2.0 [118] to create the `CalcHEP` [119] model files. As mentioned earlier, we assume $\tan\beta = 60$ and a low reheating temperature of $T_{\rm R} = 150\,\text{GeV}$.

From our discussion we see that we have 4 free parameters to determine the DM in our model:

1. the scalar flavon soft-mass $\widetilde{m}_\phi$,
2. the flavor breaking scale Λ_ϕ,
3. the coupling β_1 in eq. (3.3), and
4. the coupling β_4 in eq. (3.3).

We fix $10^{-6} \leq \beta_1, \beta_4 \leq 10^{-4}$ and $20\,\text{TeV} \leq \widetilde{m}_\phi, \Lambda_\phi \leq 1000\,\text{TeV}$. These bounds for the couplings β_1, β_4 respect the perturbativity of all the couplings β_i (cf. eq. (4.6)).

In figure 5 we show the prediction for DM relic abundance as a function of β_1 and β_4, for $\Lambda_\phi > \widetilde{m}_\phi$ (figure 5(a)), $\widetilde{m}_\phi = \Lambda_\phi$ (figure 5(b)), and $\widetilde{m}_\phi < \Lambda_\phi$ (figure 5(c)). The unshaded region indicates the excluded parameter space where too much DM is produced. We see that all plots in figure 5 exhibit similar behavior. It is possible to have a coupling up to $\beta_4, \beta_1 = 10^{-4}$, but not at the same time. This is consistent with the fact that freeze-in normally requires small couplings [114]. Furthermore, the abundance increases as we increase either β_1 or β_4, which is consistent with the fact that the DM relic abundance increases with $\langle \sigma v \rangle$.

Figure 6 shows the predicted DM relic abundance as a function of $\widetilde{m}_\phi$ and Λ_ϕ for $\beta_1 > \beta_4$ (figure 6(a)), $\beta_1 = \beta_4$ (figure 6(b)), and $\beta_1 < \beta_4$ (figure 6(c)). The unshaded space represents the excluded parameter space. We observe a similar behavior for the three plots in figure 6. The DM abundance decreases if either $\widetilde{m}_\phi$ or Λ_ϕ grows. Furthermore, a soft-mass of $m_\phi = 20\,\text{TeV}$ and a simultaneous flavon breaking-scale $\Lambda_\phi = 20\,\text{TeV}$ is excluded in all cases for the chosen values of other parameters.

Finally, in figure 7 we show the correlation between the minimum scalar flavon mass $m_{\phi_{\rm MIN}}$ and DM mass $m_{\rm DM}$ for fixed values of $\beta_1 > \beta_4$ (figure 7(a)), $\beta_1 = \beta_4$ (figure 7(b)), and $\beta_1 < \beta_4$ (figure 7(c)). By comparing figures 6 and 7, we find that for a given value of the

[4] If we had chosen high enough reheating temperatures, then the $A-$terms of eq. (2.20) would have dominated the production of DM. In this case, the connection between DM and flavor parameters is weakened.

JHEP12(2024)091

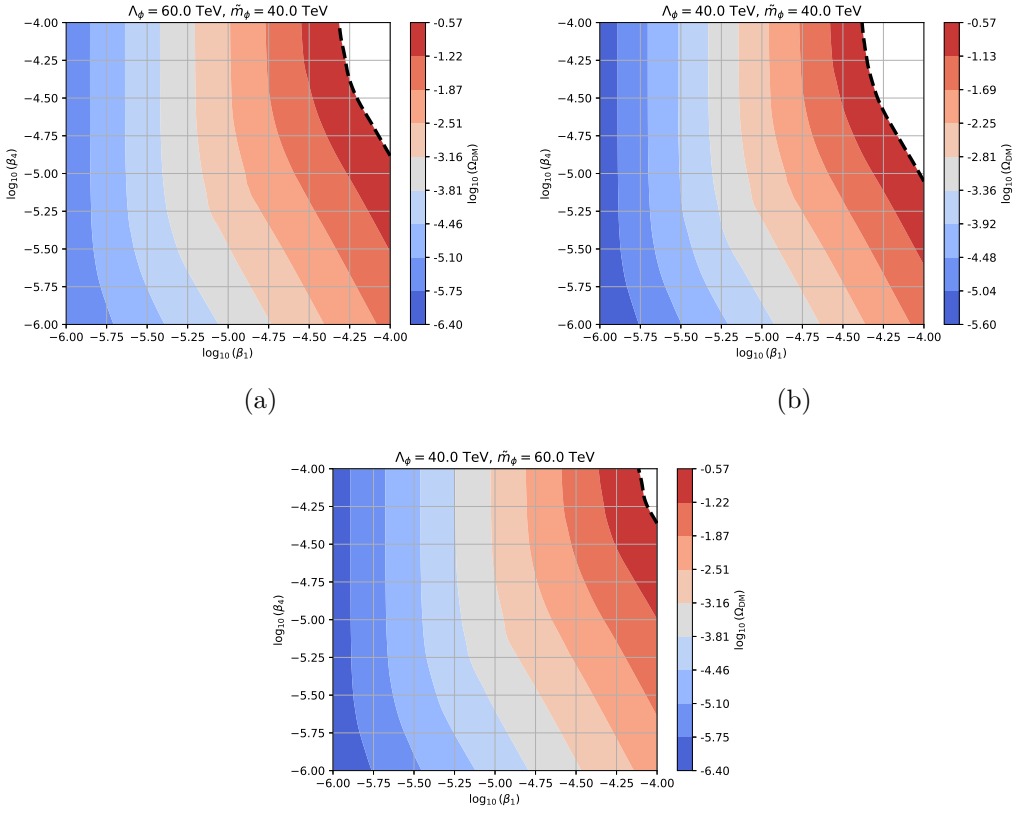

Figure 5. Predicted DM relic abundance as a function of $\log_{10}(\beta_1)$ and $\log_{10}(\beta_4)$ with fixed values of $\widetilde{m}_\phi$ and Λ_ϕ at some benchmark values. We choose $T_{\rm R} = 150\,\text{GeV}$. The dashed black line denotes the relic DM abundance $\Omega_{\rm DM} = 0.265$.

soft-mass $\widetilde{m}_\phi$, the minimum scalar flavon mass $m_{\phi_{\rm MIN}}$ constrained by the DM relic abundance can be derived. We see that the scalar flavon mass can be as low as $\sim 63\,\text{TeV}$ for all cases illustrated in figure 7. Moreover, the DM mass can be as low as $\sim 16\,\text{GeV}$ for $\beta_1 = 6 \times 10^{-5}$ and $\beta_4 = 10^{-4}$. Note that the big mass splitting between the mediator and the DM, as seen in figure 7, is a consequence from the big soft-mass contribution from supersymmetry breaking to the mediator mass (see discussion before eq. (5.4)). A mechanism for supersymmetry breakdown is beyond the scope of this work and must be explored elsewhere.

To conclude this section, let us comment on the bounds from direct detection for this model. The energy-independent cross section for the scattering process $\psi\, e^- \to \psi\, e^-$ between a DM particle ψ and the electron e^- is given by (cf. [120, Equations (9) and (10)])

$$\bar{\sigma}_{e\psi} \;=\; \frac{\mu_{e\,\psi}^2}{\pi}\,\frac{\alpha^2\beta^2}{(q_{\rm ref}^2 - m_\phi^2)^2}\,, \tag{5.5}$$

where $q_{\rm ref} = \alpha_{EM} m_e$ is the reference momentum (with the electromagnetic fine-structure constant $\alpha_{EM} \approx 1/137$ and the electron mass m_e), $\mu_{e\,\psi}$ denotes the reduced mass of the DM candidate and the electron, α and β are respectively the mediator-electron and mediator-DM

JHEP12(2024)091

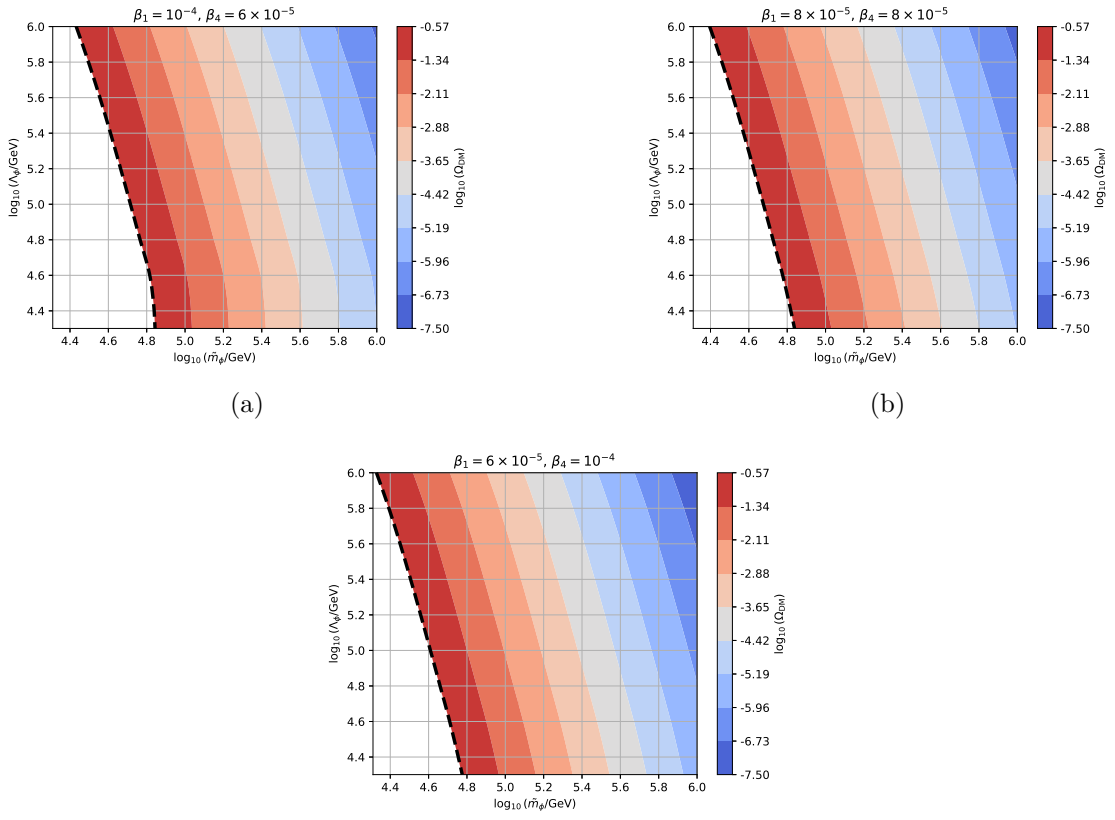

(a) (b)

(c)

Figure 6. Predicted DM relic abundance as a function of $\log_{10}(\widetilde{m}_\phi/\text{GeV})$ and $\log_{10}(\Lambda_\phi/\text{GeV})$ with fixed values of β_1 and β_4 at some benchmark values. We choose $T_{\text{R}} = 150\,\text{GeV}$. The dashed black line denotes the relic DM abundance $\Omega_{\text{DM}} = 0.265$.

couplings, and m_ϕ is the mediator mass. Assuming $m_\psi = 1\,\text{GeV}$, $\alpha = 10^{-3}$, $\beta = 10^{-4}$ and $m_\phi = 20\,\text{TeV}$ (consistent with couplings shown in eq. (4.5) and figures 5–7), we obtain

$$\bar{\sigma}_{e\psi} \sim 10^{-66}\,\text{cm}^2\,, \tag{5.6}$$

which is unfortunately found below the direct detection bounds from XENON1T [121], for a DM mass of 1 GeV. It is known that the detection bounds can change depending on the energy-dependence of the cross section, or on the form of the so-called DM form factor $F_{\text{DM}}(q)$. However, we do not expect the energy-independent cross section in eq. (5.6) to significantly increase to become experimentally detectable (see [122, figure 3]). This implies that the DM features of our model require new experimental settings.

6 Conclusion

We constructed a flavor model based on the finite modular group $\Gamma_3 \cong A_4$ that simultaneously explains the flavor parameters in the lepton sector and accounts for the observed DM relic abundance in the Universe. The 12 lepton flavor parameters are determined by 8 real

JHEP12(2024)091

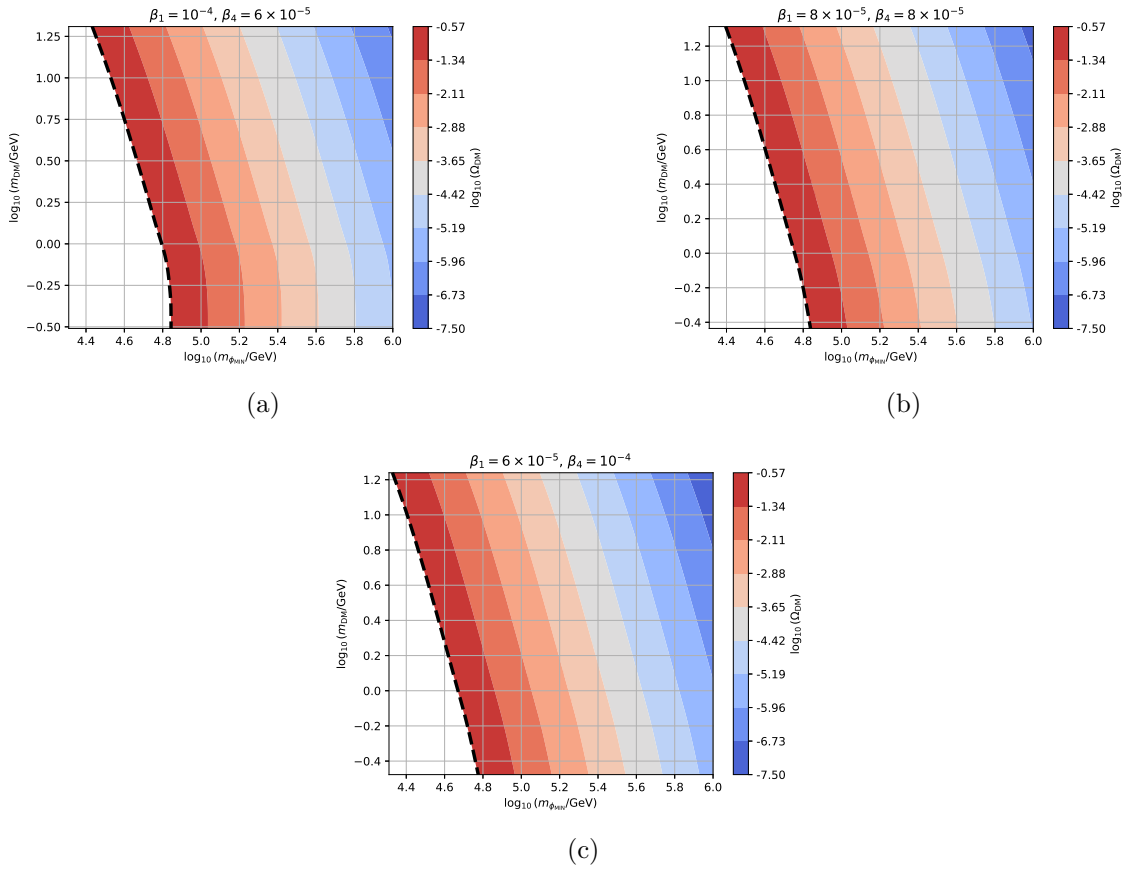

Figure 7. Predicted DM relic abundance as a function of the minimum mediator scalar flavon mass $\log_{10}(m_{\phi_{\rm MIN}}/{\rm GeV})$ and DM mass $\log_{10}(m_{\rm DM}/{\rm GeV})$ for fixed β_1 and β_4 at some benchmark values. We fix $T_{\rm R} = 150$ GeV. The dashed black line denotes the relic DM abundance $\Omega_{\rm DM} = 0.265$.

parameters: the two components of the modulus VEV, the four flavon VEVs, $\langle\phi_i\rangle$, and two dimensionful parameters that set the mass scales of charged-lepton and neutrino masses. We identify a DM candidate composed of the fermionic parts of the flavon superfields and the driving superfields. The mediator is the scalar part of the flavon superfield which interacts with the charged-lepton sector of the SM. We obtain a good fit to the lepton flavor parameters (3 charged lepton masses, 3 mixing angles, 1 $\mathcal{CP}$ phase, 2 neutrino squared mass differences) with $\chi^2 = 0.08$ for an inverted-hierarchy neutrino spectrum. The lepton flavor fit fixes the couplings of the charged leptons to the DM mediator as well as the flavon VEVs $\langle\phi_i\rangle$. These VEVs satisfy the F-term equations to retain supersymmetry at high energies, determining thereby the coupling between our DM candidate and the mediator. Interestingly, our model exhibits 4 additional degrees of freedom that are left free and serve to achieve a DM relic abundance which does not exceed the observed value $\Omega_{\rm CDM} = 0.265$. These parameters are 2 dimensionless couplings β_1, β_4, the flavor breaking scale Λ_ϕ, and the soft-mass for the flavon $\widetilde{m}_\phi$. We find that if the mediator mass is assumed to be much larger than the DM and the charged-lepton masses, then the appropriate DM production mechanism is freeze-in rather than freeze-out. We observe that a viable DM relic abundance can be generated in regions

JHEP12(2024)091

of the parameter space constrained by $10^{-6} \leq \beta_1, \beta_4 \leq 10^{-4}$, $20\,\text{TeV} \leq \widetilde{m}_\phi$, $\Lambda_\phi \leq 1000\,\text{TeV}$, $\tan\beta = 60$, and $T_R = 150\,\text{GeV}$.

Although some amount of tuning is necessary in our model to identify the best parameter values, we point out that it is the choice of charges and modular weights that render the right flavon superpotential, which in turn delivers the alignment of the flavon VEVs $\langle\phi_i\rangle$. Further, the phenomenologically viable value of the modulus VEV $\langle\tau\rangle$ might be achieved through mechanisms as in [97]. The flavor structure of our model, that includes the flavon superpotential, determines the properties of our DM candidate. In particular, a different choice of flavor parameters in eqs. (4.5) and (4.6), which set the flavor predictions, strongly influences the mass and production (e.g. freeze-in vs. freeze-out) of DM in our model.

As a feasible outlook of our findings, it would be interesting to study the possibility of applying this new scenario in top-down models such as [88]. Furthermore, as the flavor sector of our model only accounts for leptons, it should be extended to the quark sector as a first direct step. In addition, in our scenario we expect the DM-nucleon cross section to be too small to be directly compared with LUX [123], DEAP-3600 [124], PandaX-II [125], DarkSide [126], EDELWEISS [127] and any other currently envisaged experiments of this type. One should hence explore additional indirect evidence of our proposal. We leave these intriguing questions for upcoming work.

Acknowledgments

The work of M.-C.C. and V.K.-P. was partially supported by the U.S. National Science Foundation under Grant No. PHY-1915005. The work of S.R.-S. was partly supported by UNAM-PAPIIT grant IN113223 and Marcos Moshinsky Foundation. This work was also supported by UC-MEXUS-CONACyT grant No. CN-20-38. V.K.-P. would like to thank Kevork N. Abazajian, Max Fieg, Xueqi Li, Xiang-Gan Liu, Gopolang Mohlabeng, Michael Ratz and Miša Toman for fruitful discussions. M-C.C.and V.K.-P. would also like to thank Instituto de Física, UNAM, for the hospitality during their visit. A.B. would like to thank the Department of Physics and Astronomy at UCI for the hospitality during his visit. V.K.-P. also thanks the opportunity to use the cluster at Instituto de Física, UNAM. This work utilized the infrastructure for high-performance and high-throughput computing, research data storage and analysis, and scientific software tool integration built, operated, and updated by the Research Cyberinfrastructure Center (RCIC) at the University of California, Irvine (UCI). The RCIC provides cluster-based systems, application software, and scalable storage to directly support the UCI research community. https://rcic.uci.edu

Data Availability Statement. This article has no associated data or the data will not be deposited.

Code Availability Statement. This article has no associated code or the code will not be deposited.

JHEP12(2024)091

References

[1] G. Altarelli and F. Feruglio, *Discrete flavor symmetries and models of neutrino mixing*, *Rev. Mod. Phys.* **82** (2010) 2701 [arXiv:1002.0211] [INSPIRE].

[2] H. Ishimori et al., *Non-Abelian discrete symmetries in particle physics*, *Prog. Theor. Phys. Suppl.* **183** (2010) 1 [arXiv:1003.3552] [INSPIRE].

[3] D. Hernández and A.Y. Smirnov, *Lepton mixing and discrete symmetries*, *Phys. Rev. D* **86** (2012) 053014 [arXiv:1204.0445] [INSPIRE].

[4] S.F. King and C. Luhn, *Neutrino mass and mixing with discrete symmetry*, *Rept. Prog. Phys.* **76** (2013) 056201 [arXiv:1301.1340] [INSPIRE].

[5] S.F. King et al., *Neutrino mass and mixing: from theory to experiment*, *New J. Phys.* **16** (2014) 045018 [arXiv:1402.4271] [INSPIRE].

[6] S.F. King, *Unified models of neutrinos, flavour and CP violation*, *Prog. Part. Nucl. Phys.* **94** (2017) 217 [arXiv:1701.04413] [INSPIRE].

[7] F. Feruglio and A. Romanino, *Lepton flavor symmetries*, *Rev. Mod. Phys.* **93** (2021) 015007 [arXiv:1912.06028] [INSPIRE].

[8] G. Altarelli and F. Feruglio, *Tri-bimaximal neutrino mixing, A_4 and the modular symmetry*, *Nucl. Phys. B* **741** (2006) 215 [hep-ph/0512103] [INSPIRE].

[9] F. Feruglio, C. Hagedorn and L. Merlo, *Vacuum alignment in SUSY A_4 models*, *JHEP* **03** (2010) 084 [arXiv:0910.4058] [INSPIRE].

[10] G.-J. Ding, S.F. King, C. Luhn and A.J. Stuart, *Spontaneous CP violation from vacuum alignment in S_4 models of leptons*, *JHEP* **05** (2013) 084 [arXiv:1303.6180] [INSPIRE].

[11] C.-C. Li and G.-J. Ding, *Generalised CP and trimaximal TM_1 lepton mixing in S_4 family symmetry*, *Nucl. Phys. B* **881** (2014) 206 [arXiv:1312.4401] [INSPIRE].

[12] Y. Muramatsu, T. Nomura and Y. Shimizu, *Mass limit for light flavon with residual Z_3 symmetry*, *JHEP* **03** (2016) 192 [arXiv:1601.04788] [INSPIRE].

[13] S.F. King and Y.-L. Zhou, *Littlest mu-tau seesaw*, *JHEP* **05** (2019) 217 [arXiv:1901.06877] [INSPIRE].

[14] A.E. Cárcamo Hernández and S.F. King, *Littlest inverse seesaw model*, *Nucl. Phys. B* **953** (2020) 114950 [arXiv:1903.02565] [INSPIRE].

[15] M.-C. Chen et al., *Quasi-eclectic modular flavor symmetries*, *Phys. Lett. B* **824** (2022) 136843 [arXiv:2108.02240] [INSPIRE].

[16] M. Hirsch, S. Morisi, E. Peinado and J.W.F. Valle, *Discrete dark matter*, *Phys. Rev. D* **82** (2010) 116003 [arXiv:1007.0871] [INSPIRE].

[17] X.-G. He et al., *Scalar dark matter explanation of the excess in the Belle II $B^+ \to K^+ +$ invisible measurement*, *JHEP* **07** (2024) 168 [arXiv:2403.12485] [INSPIRE].

[18] H. Acaroğlu et al., *Flavoured Majorana dark matter then and now: from freeze-out scenarios to LHC signatures*, *JHEP* **06** (2024) 179 [arXiv:2312.09274] [INSPIRE].

[19] H. Acaroğlu and M. Blanke, *Tasting flavoured Majorana dark matter*, *JHEP* **05** (2022) 086 [arXiv:2109.10357] [INSPIRE].

[20] F. Feruglio, *Are neutrino masses modular forms?*, in *From my vast repertoire...: Guido Altarelli's legacy*, A. Levy et al. eds., (2019), p. 227–266 [DOI:10.1142/9789813238053_0012] [arXiv:1706.08749] [INSPIRE].

JHEP12(2024)091

[21] J.C. Criado and F. Feruglio, *Modular invariance faces precision neutrino data*, *SciPost Phys.* **5** (2018) 042 [arXiv:1807.01125] [INSPIRE].

[22] T. Kobayashi, K. Tanaka and T.H. Tatsuishi, *Neutrino mixing from finite modular groups*, *Phys. Rev. D* **98** (2018) 016004 [arXiv:1803.10391] [INSPIRE].

[23] F.J. de Anda, S.F. King and E. Perdomo, SU(()*5) grand unified theory with* A_4 *modular symmetry*, *Phys. Rev. D* **101** (2020) 015028 [arXiv:1812.05620] [INSPIRE].

[24] H. Okada and M. Tanimoto, *CP violation of quarks in* A_4 *modular invariance*, *Phys. Lett. B* **791** (2019) 54 [arXiv:1812.09677] [INSPIRE].

[25] G.-J. Ding, S.F. King and X.-G. Liu, *Neutrino mass and mixing with* A_5 *modular symmetry*, *Phys. Rev. D* **100** (2019) 115005 [arXiv:1903.12588] [INSPIRE].

[26] T. Kobayashi et al., A_4 *lepton flavor model and modulus stabilization from* S_4 *modular symmetry*, *Phys. Rev. D* **100** (2019) 115045 [*Erratum ibid.* **101** (2020) 039904] [arXiv:1909.05139] [INSPIRE].

[27] T. Asaka, Y. Heo, T.H. Tatsuishi and T. Yoshida, *Modular* A_4 *invariance and leptogenesis*, *JHEP* **01** (2020) 144 [arXiv:1909.06520] [INSPIRE].

[28] X.-G. Liu and G.-J. Ding, *Neutrino masses and mixing from double covering of finite modular groups*, *JHEP* **08** (2019) 134 [arXiv:1907.01488] [INSPIRE].

[29] G.-J. Ding and S.F. King, *Neutrino mass and mixing with modular symmetry*, *Rept. Prog. Phys.* **87** (2024) 084201 [arXiv:2311.09282] [INSPIRE].

[30] T. Kobayashi et al., *Modular* A_4 *invariance and neutrino mixing*, *JHEP* **11** (2018) 196 [arXiv:1808.03012] [INSPIRE].

[31] P.P. Novichkov, J.T. Penedo, S.T. Petcov and A.V. Titov, *Modular* A_5 *symmetry for flavour model building*, *JHEP* **04** (2019) 174 [arXiv:1812.02158] [INSPIRE].

[32] P.P. Novichkov, J.T. Penedo, S.T. Petcov and A.V. Titov, *Modular* S_4 *models of lepton masses and mixing*, *JHEP* **04** (2019) 005 [arXiv:1811.04933] [INSPIRE].

[33] P.P. Novichkov, S.T. Petcov and M. Tanimoto, *Trimaximal neutrino mixing from modular* A_4 *invariance with residual symmetries*, *Phys. Lett. B* **793** (2019) 247 [arXiv:1812.11289] [INSPIRE].

[34] J.T. Penedo and S.T. Petcov, *Lepton masses and mixing from modular* S_4 *symmetry*, *Nucl. Phys. B* **939** (2019) 292 [arXiv:1806.11040] [INSPIRE].

[35] J.C. Criado, F. Feruglio and S.J.D. King, *Modular invariant models of lepton masses at levels 4 and 5*, *JHEP* **02** (2020) 001 [arXiv:1908.11867] [INSPIRE].

[36] G.-J. Ding, S.F. King and X.-G. Liu, *Modular* A_4 *symmetry models of neutrinos and charged leptons*, *JHEP* **09** (2019) 074 [arXiv:1907.11714] [INSPIRE].

[37] T. Kobayashi et al., *New* A_4 *lepton flavor model from* S_4 *modular symmetry*, *JHEP* **02** (2020) 097 [arXiv:1907.09141] [INSPIRE].

[38] G.-J. Ding, S.F. King, C.-C. Li and Y.-L. Zhou, *Modular invariant models of leptons at level 7*, *JHEP* **08** (2020) 164 [arXiv:2004.12662] [INSPIRE].

[39] P.P. Novichkov, J.T. Penedo and S.T. Petcov, *Double cover of modular* S_4 *for flavour model building*, *Nucl. Phys. B* **963** (2021) 115301 [arXiv:2006.03058] [INSPIRE].

[40] X. Wang, B. Yu and S. Zhou, *Double covering of the modular* A_5 *group and lepton flavor mixing in the minimal seesaw model*, *Phys. Rev. D* **103** (2021) 076005 [arXiv:2010.10159] [INSPIRE].

JHEP12(2024)091

[41] C.-C. Li, X.-G. Liu and G.-J. Ding, *Modular symmetry at level 6 and a new route towards finite modular groups*, *JHEP* **10** (2021) 238 [arXiv:2108.02181] [INSPIRE].

[42] T. Kobayashi et al., *Modular S_3-invariant flavor model in* SU(()*5) grand unified theory*, *PTEP* **2020** (2020) 053B05 [arXiv:1906.10341] [INSPIRE].

[43] G.-J. Ding, F. Feruglio and X.-G. Liu, *Automorphic forms and fermion masses*, *JHEP* **01** (2021) 037 [arXiv:2010.07952] [INSPIRE].

[44] J.-N. Lu, X.-G. Liu and G.-J. Ding, *Modular symmetry origin of texture zeros and quark lepton unification*, *Phys. Rev. D* **101** (2020) 115020 [arXiv:1912.07573] [INSPIRE].

[45] S.J.D. King and S.F. King, *Fermion mass hierarchies from modular symmetry*, *JHEP* **09** (2020) 043 [arXiv:2002.00969] [INSPIRE].

[46] X.-G. Liu, C.-Y. Yao and G.-J. Ding, *Modular invariant quark and lepton models in double covering of S_4 modular group*, *Phys. Rev. D* **103** (2021) 056013 [arXiv:2006.10722] [INSPIRE].

[47] H. Okada and M. Tanimoto, *Modular invariant flavor model of A_4 and hierarchical structures at nearby fixed points*, *Phys. Rev. D* **103** (2021) 015005 [arXiv:2009.14242] [INSPIRE].

[48] P. Chen, G.-J. Ding and S.F. King, SU(()*5) GUTs with A_4 modular symmetry*, *JHEP* **04** (2021) 239 [arXiv:2101.12724] [INSPIRE].

[49] G.-J. Ding, S.F. King and J.-N. Lu, *SO(10) models with A_4 modular symmetry*, *JHEP* **11** (2021) 007 [arXiv:2108.09655] [INSPIRE].

[50] Y. Zhao and H.-H. Zhang, *Adjoint* SU(()*5) GUT model with modular S_4 symmetry*, *JHEP* **03** (2021) 002 [arXiv:2101.02266] [INSPIRE].

[51] C. Arriaga-Osante, X.-G. Liu and S. Ramos-Sánchez, *Quark and lepton modular models from the binary dihedral flavor symmetry*, *JHEP* **05** (2024) 119 [arXiv:2311.10136] [INSPIRE].

[52] S. Kikuchi et al., *Quark mass hierarchies and CP violation in $A_4 \times A_4 \times A_4$ modular symmetric flavor models*, *JHEP* **07** (2023) 134 [arXiv:2302.03326] [INSPIRE].

[53] S. Kikuchi et al., *Sp(6,Z) modular symmetry in flavor structures: quark flavor models and Siegel modular forms for $\widetilde{\Delta}(96)$*, *JHEP* **04** (2024) 045 [arXiv:2310.17978] [INSPIRE].

[54] F. Feruglio, V. Gherardi, A. Romanino and A. Titov, *Modular invariant dynamics and fermion mass hierarchies around $\tau = i$*, *JHEP* **05** (2021) 242 [arXiv:2101.08718] [INSPIRE].

[55] F. Feruglio, *Universal predictions of modular invariant flavor models near the self-dual point*, *Phys. Rev. Lett.* **130** (2023) 101801 [arXiv:2211.00659] [INSPIRE].

[56] S.T. Petcov and M. Tanimoto, *A_4 modular flavour model of quark mass hierarchies close to the fixed point $\tau = \omega$*, *Eur. Phys. J. C* **83** (2023) 579 [arXiv:2212.13336] [INSPIRE].

[57] Y. Abe, T. Higaki, J. Kawamura and T. Kobayashi, *Quark masses and CKM hierarchies from S_4' modular flavor symmetry*, *Eur. Phys. J. C* **83** (2023) 1140 [arXiv:2301.07439] [INSPIRE].

[58] F. Feruglio, *Fermion masses, critical behavior and universality*, *JHEP* **03** (2023) 236 [arXiv:2302.11580] [INSPIRE].

[59] T. Nomura and H. Okada, *A modular A_4 symmetric model of dark matter and neutrino*, *Phys. Lett. B* **797** (2019) 134799 [arXiv:1904.03937] [INSPIRE].

[60] M.K. Behera, S. Singirala, S. Mishra and R. Mohanta, *A modular A_4 symmetric scotogenic model for neutrino mass and dark matter*, *J. Phys. G* **49** (2022) 035002 [arXiv:2009.01806] [INSPIRE].

JHEP12(2024)091

[61] P.T.P. Hutauruk, D.W. Kang, J. Kim and H. Okada, *Muon $g-2$, dark matter, and neutrino mass explanations in a modular A_4 symmetry*, *Phys. Dark Univ.* **44** (2024) 101440 [arXiv:2012.11156] [INSPIRE].

[62] T. Kobayashi, H. Okada and Y. Orikasa, *Dark matter stability at fixed points in a modular A_4 symmetry*, *Phys. Dark Univ.* **37** (2022) 101080 [arXiv:2111.05674] [INSPIRE].

[63] X. Zhang and S. Zhou, *Inverse seesaw model with a modular S_4 symmetry: lepton flavor mixing and warm dark matter*, *JCAP* **09** (2021) 043 [arXiv:2106.03433] [INSPIRE].

[64] T. Kobayashi, S. Nagamoto and S. Uemura, *Modular symmetry in magnetized/intersecting D-brane models*, *PTEP* **2017** (2017) 023B02 [arXiv:1608.06129] [INSPIRE].

[65] T. Kobayashi et al., *Modular symmetry and non-Abelian discrete flavor symmetries in string compactification*, *Phys. Rev. D* **97** (2018) 116002 [arXiv:1804.06644] [INSPIRE].

[66] T. Kobayashi and S. Tamba, *Modular forms of finite modular subgroups from magnetized D-brane models*, *Phys. Rev. D* **99** (2019) 046001 [arXiv:1811.11384] [INSPIRE].

[67] Y. Kariyazono et al., *Modular symmetry anomaly in magnetic flux compactification*, *Phys. Rev. D* **100** (2019) 045014 [arXiv:1904.07546] [INSPIRE].

[68] K. Hoshiya et al., *Classification of three-generation models by orbifolding magnetized $T^2 \times T^2$*, *PTEP* **2021** (2021) 033B05 [arXiv:2012.00751] [INSPIRE].

[69] S. Kikuchi et al., *Revisiting modular symmetry in magnetized torus and orbifold compactifications*, *Phys. Rev. D* **102** (2020) 105010 [arXiv:2005.12642] [INSPIRE].

[70] S. Kikuchi et al., *Modular symmetry by orbifolding magnetized $T^2 \times T^2$: realization of double cover of Γ_N*, *JHEP* **11** (2020) 101 [arXiv:2007.06188] [INSPIRE].

[71] H. Ohki, S. Uemura and R. Watanabe, *Modular flavor symmetry on a magnetized torus*, *Phys. Rev. D* **102** (2020) 085008 [arXiv:2003.04174] [INSPIRE].

[72] Y. Almumin et al., *Metaplectic flavor symmetries from magnetized tori*, *JHEP* **05** (2021) 078 [arXiv:2102.11286] [INSPIRE].

[73] S. Kikuchi, T. Kobayashi and H. Uchida, *Modular flavor symmetries of three-generation modes on magnetized toroidal orbifolds*, *Phys. Rev. D* **104** (2021) 065008 [arXiv:2101.00826] [INSPIRE].

[74] Y. Tatsuta, *Modular symmetry and zeros in magnetic compactifications*, *JHEP* **10** (2021) 054 [arXiv:2104.03855] [INSPIRE].

[75] S. Kikuchi et al., *Modular symmetry anomaly and nonperturbative neutrino mass terms in magnetized orbifold models*, *Phys. Rev. D* **105** (2022) 116002 [arXiv:2202.05425] [INSPIRE].

[76] S. Kikuchi, T. Kobayashi, K. Nasu and H. Uchida, *Classifications of magnetized T^4 and T^4/Z_2 orbifold models*, *JHEP* **08** (2022) 256 [arXiv:2203.01649] [INSPIRE].

[77] S. Kikuchi et al., *Number of zero-modes on magnetized T^4/Z_N orbifolds analyzed by modular transformation*, *JHEP* **06** (2023) 013 [arXiv:2211.07813] [INSPIRE].

[78] A. Baur, H.P. Nilles, A. Trautner and P.K.S. Vaudrevange, *Unification of flavor, CP, and modular symmetries*, *Phys. Lett. B* **795** (2019) 7 [arXiv:1901.03251] [INSPIRE].

[79] A. Baur, H.P. Nilles, A. Trautner and P.K.S. Vaudrevange, *A string theory of flavor and CP*, *Nucl. Phys. B* **947** (2019) 114737 [arXiv:1908.00805] [INSPIRE].

[80] H.P. Nilles, S. Ramos-Sánchez and P.K.S. Vaudrevange, *Lessons from eclectic flavor symmetries*, *Nucl. Phys. B* **957** (2020) 115098 [arXiv:2004.05200] [INSPIRE].

JHEP12(2024)091

[81] H.P. Nilles, S. Ramos-Sánchez and P.K.S. Vaudrevange, *Eclectic flavor scheme from ten-dimensional string theory — I. Basic results*, *Phys. Lett. B* **808** (2020) 135615 [arXiv:2006.03059] [INSPIRE].

[82] A. Baur et al., *The eclectic flavor symmetry of the Z_2 orbifold*, *JHEP* **02** (2021) 018 [arXiv:2008.07534] [INSPIRE].

[83] H.P. Nilles, S. Ramos-Sánchez and P.K.S. Vaudrevange, *Eclectic flavor scheme from ten-dimensional string theory — II detailed technical analysis*, *Nucl. Phys. B* **966** (2021) 115367 [arXiv:2010.13798] [INSPIRE].

[84] A. Baur et al., *Siegel modular flavor group and CP from string theory*, *Phys. Lett. B* **816** (2021) 136176 [arXiv:2012.09586] [INSPIRE].

[85] A. Baur et al., *Completing the eclectic flavor scheme of the Z_2 orbifold*, *JHEP* **06** (2021) 110 [arXiv:2104.03981] [INSPIRE].

[86] H.P. Nilles, S. Ramos-Sánchez, A. Trautner and P.K.S. Vaudrevange, *Orbifolds from Sp(4,Z) and their modular symmetries*, *Nucl. Phys. B* **971** (2021) 115534 [arXiv:2105.08078] [INSPIRE].

[87] A. Baur et al., *Top-down anatomy of flavor symmetry breakdown*, *Phys. Rev. D* **105** (2022) 055018 [arXiv:2112.06940] [INSPIRE].

[88] A. Baur et al., *The first string-derived eclectic flavor model with realistic phenomenology*, *JHEP* **09** (2022) 224 [arXiv:2207.10677] [INSPIRE].

[89] A. Baur et al., *The eclectic flavor symmetries of T^2/Z_K orbifolds*, *JHEP* **09** (2024) 159 [arXiv:2405.20378] [INSPIRE].

[90] H.P. Nilles, S. Ramos-Sánchez and P.K.S. Vaudrevange, *Eclectic flavor groups*, *JHEP* **02** (2020) 045 [arXiv:2001.01736] [INSPIRE].

[91] A. Font, L.E. Ibanez, D. Lust and F. Quevedo, *Supersymmetry breaking from duality invariant gaugino condensation*, *Phys. Lett. B* **245** (1990) 401 [INSPIRE].

[92] H.P. Nilles and M. Olechowski, *Gaugino condensation and duality invariance*, *Phys. Lett. B* **248** (1990) 268 [INSPIRE].

[93] M. Cvetic et al., *Target space duality, supersymmetry breaking and the stability of classical string vacua*, *Nucl. Phys. B* **361** (1991) 194 [INSPIRE].

[94] S. Kachru, R. Kallosh, A.D. Linde and S.P. Trivedi, *De Sitter vacua in string theory*, *Phys. Rev. D* **68** (2003) 046005 [hep-th/0301240] [INSPIRE].

[95] K.A. Intriligator, N. Seiberg and D. Shih, *Dynamical SUSY breaking in meta-stable vacua*, *JHEP* **04** (2006) 021 [hep-th/0602239] [INSPIRE].

[96] J.M. Leedom, N. Righi and A. Westphal, *Heterotic de Sitter beyond modular symmetry*, *JHEP* **02** (2023) 209 [arXiv:2212.03876] [INSPIRE].

[97] V. Knapp-Pérez et al., *Matter matters in moduli fixing and modular flavor symmetries*, *Phys. Lett. B* **844** (2023) 138106 [arXiv:2304.14437] [INSPIRE].

[98] Particle Data Group collaboration, *Review of particle physics*, *Phys. Rev. D* **110** (2024) 030001 [INSPIRE].

[99] T. Nomura, Y. Shimizu and T. Takahashi, *Flavino dark matter in a non-Abelian discrete flavor model*, *JHEP* **09** (2024) 036 [arXiv:2405.14163] [INSPIRE].

JHEP12(2024)091

[100] X.-G. Liu, C.-Y. Yao, B.-Y. Qu and G.-J. Ding, *Half-integral weight modular forms and application to neutrino mass models*, *Phys. Rev. D* **102** (2020) 115035 [arXiv:2007.13706] [INSPIRE].

[101] X.-G. Liu and G.-J. Ding, *Modular flavor symmetry and vector-valued modular forms*, *JHEP* **03** (2022) 123 [arXiv:2112.14761] [INSPIRE].

[102] M.-C. Chen, S. Ramos-Sánchez and M. Ratz, *A note on the predictions of models with modular flavor symmetries*, *Phys. Lett. B* **801** (2020) 135153 [arXiv:1909.06910] [INSPIRE].

[103] G.-J. Ding, X.-G. Liu and C.-Y. Yao, *A minimal modular invariant neutrino model*, *JHEP* **01** (2023) 125 [arXiv:2211.04546] [INSPIRE].

[104] J. Terning, *Modern supersymmetry: dynamics and duality*, Oxford University Press, Oxford, U.K. (2006) [DOI:10.1093/acprof:oso/9780198567639.001.0001] [INSPIRE].

[105] I. Esteban et al., *The fate of hints: updated global analysis of three-flavor neutrino oscillations*, *JHEP* **09** (2020) 178 [arXiv:2007.14792] [INSPIRE].

[106] S. Antusch and V. Maurer, *Running quark and lepton parameters at various scales*, *JHEP* **11** (2013) 115 [arXiv:1306.6879] [INSPIRE].

[107] A. Baur, *Flavorpy 0.2.0*, Zenodo (2024). [DOI:10.5281/zenodo.11060597].

[108] PLANCK collaboration, *Planck 2018 results. VI. Cosmological parameters*, *Astron. Astrophys.* **641** (2020) A6 [*Erratum ibid.* **652** (2021) C4] [arXiv:1807.06209] [INSPIRE].

[109] KATRIN collaboration, *Direct neutrino-mass measurement with sub-electronvolt sensitivity*, *Nature Phys.* **18** (2022) 160 [arXiv:2105.08533] [INSPIRE].

[110] KAMLAND-ZEN collaboration, *Search for the Majorana nature of neutrinos in the inverted mass ordering region with KamLAND-Zen*, *Phys. Rev. Lett.* **130** (2023) 051801 [arXiv:2203.02139] [INSPIRE].

[111] GAMBIT COSMOLOGY WORKGROUP collaboration, *Strengthening the bound on the mass of the lightest neutrino with terrestrial and cosmological experiments*, *Phys. Rev. D* **103** (2021) 123508 [arXiv:2009.03287] [INSPIRE].

[112] M. D'Onofrio and K. Rummukainen, *Standard model cross-over on the lattice*, *Phys. Rev. D* **93** (2016) 025003 [arXiv:1508.07161] [INSPIRE].

[113] M. Tanimoto and K. Yamamoto, *Electron EDM arising from modulus τ in the supersymmetric modular invariant flavor models*, *JHEP* **10** (2021) 183 [arXiv:2106.10919] [INSPIRE].

[114] L.J. Hall, K. Jedamzik, J. March-Russell and S.M. West, *Freeze-in production of FIMP dark matter*, *JHEP* **03** (2010) 080 [arXiv:0911.1120] [INSPIRE].

[115] G. Bélanger et al., *micrOMEGAs5.0: freeze-in*, *Comput. Phys. Commun.* **231** (2018) 173 [arXiv:1801.03509] [INSPIRE].

[116] G. Alguero, G. Belanger, S. Kraml and A. Pukhov, *Co-scattering in micrOMEGAs: a case study for the singlet-triplet dark matter model*, *SciPost Phys.* **13** (2022) 124 [arXiv:2207.10536] [INSPIRE].

[117] G. Belanger et al., *Leptoquark manoeuvres in the dark: a simultaneous solution of the dark matter problem and the $R_{D^{(*)}}$ anomalies*, *JHEP* **02** (2022) 042 [arXiv:2111.08027] [INSPIRE].

[118] A. Alloul et al., *FeynRules 2.0 — a complete toolbox for tree-level phenomenology*, *Comput. Phys. Commun.* **185** (2014) 2250 [arXiv:1310.1921] [INSPIRE].

JHEP12(2024)091

[119] A. Belyaev, N.D. Christensen and A. Pukhov, *CalcHEP 3.4 for collider physics within and beyond the Standard Model*, *Comput. Phys. Commun.* **184** (2013) 1729 [arXiv:1207.6082] [INSPIRE].

[120] D. Bardhan et al., *Bounds on boosted dark matter from direct detection: the role of energy-dependent cross sections*, *Phys. Rev. D* **107** (2023) 015010 [arXiv:2208.09405] [INSPIRE].

[121] XENON collaboration, *Light dark matter search with ionization signals in XENON1T*, *Phys. Rev. Lett.* **123** (2019) 251801 [arXiv:1907.11485] [INSPIRE].

[122] DAMIC collaboration, *Constraints on light dark matter particles interacting with electrons from DAMIC at SNOLAB*, *Phys. Rev. Lett.* **123** (2019) 181802 [arXiv:1907.12628] [INSPIRE].

[123] LUX collaboration, *Results of a search for sub-GeV dark matter using 2013 LUX data*, *Phys. Rev. Lett.* **122** (2019) 131301 [arXiv:1811.11241] [INSPIRE].

[124] DEAP collaboration, *Search for dark matter with a 231-day exposure of liquid argon using DEAP-3600 at SNOLAB*, *Phys. Rev. D* **100** (2019) 022004 [arXiv:1902.04048] [INSPIRE].

[125] PandaX-II collaboration, *Dark matter results from 54-ton-day exposure of PandaX-II experiment*, *Phys. Rev. Lett.* **119** (2017) 181302 [arXiv:1708.06917] [INSPIRE].

[126] DarkSide collaboration, *Low-mass dark matter search with the DarkSide-50 experiment*, *Phys. Rev. Lett.* **121** (2018) 081307 [arXiv:1802.06994] [INSPIRE].

[127] EDELWEISS collaboration, *Searching for low-mass dark matter particles with a massive Ge bolometer operated above-ground*, *Phys. Rev. D* **99** (2019) 082003 [arXiv:1901.03588] [INSPIRE].

JHEP12(2024)091